Supplement of

A long-term gridded dataset of the vegetation–atmosphere decoupling coefficient across the contiguous United States, 1982–2020

Jinran Xiong et al.

Correspondence to: Yu Feng (yufeng@eitech.edu.cn)

Contents of this file

Figure S1 to S12

Table S1 to S3

Figure S1. Spatial locations of compliant sites from AmeriFlux.

A total of 74 sites were included in the study based on the selected criteria. Different colors represent different PFTs, and the size of the circles is proportional to the number of local sites to avoid overlap.

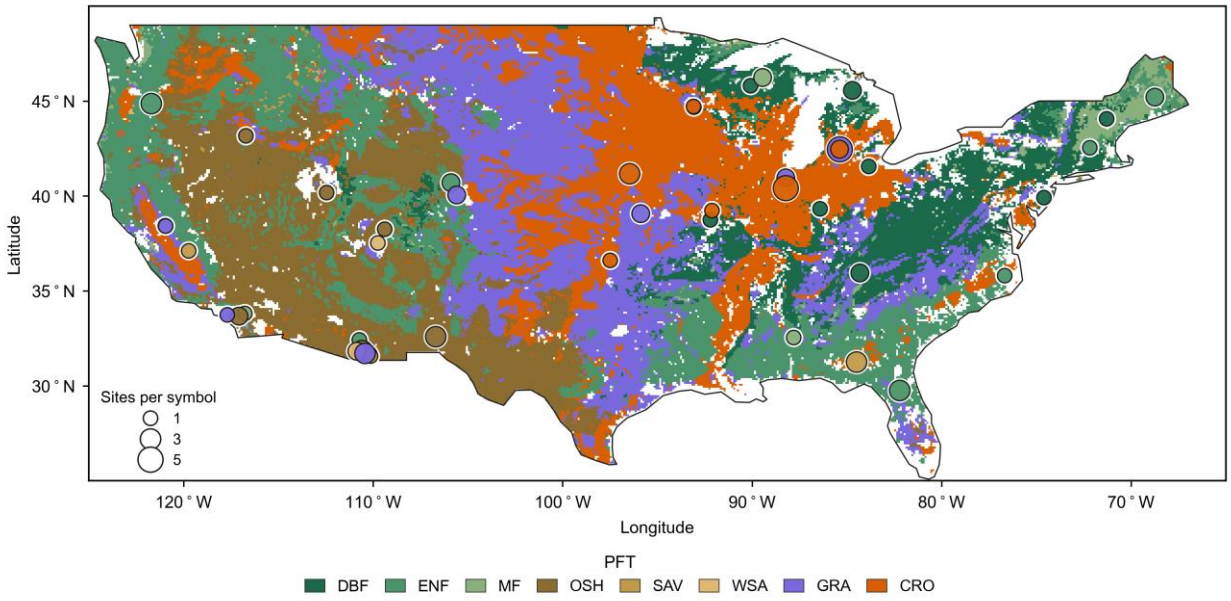


Figure S2. Representative empirical age-height relationship mapping within a selected 0.1° grid cell. Light blue points represent raw pixel-level observations (0.001° resolution) pairing GAMI forest stand age with the baseline canopy height. The solid red line denotes the calculated mean canopy height for each specific age, serving as the localized lookup table for dynamic height reconstruction. The red shaded region illustrates the ±1 standard deviation, demonstrating the distribution and uncertainty of the observational data.

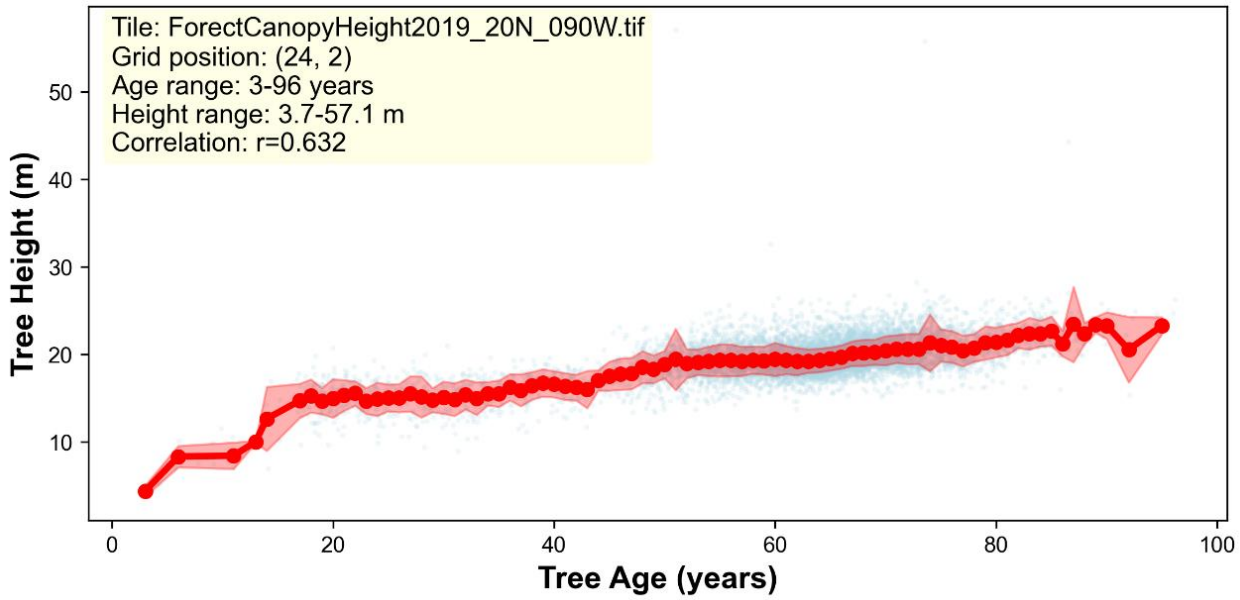
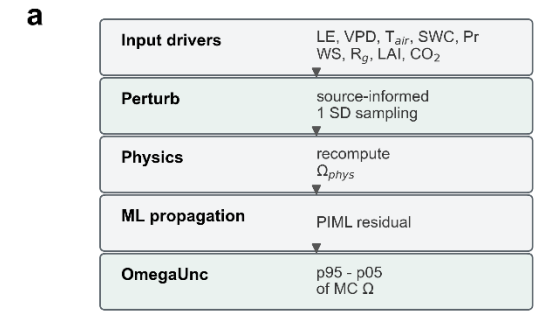


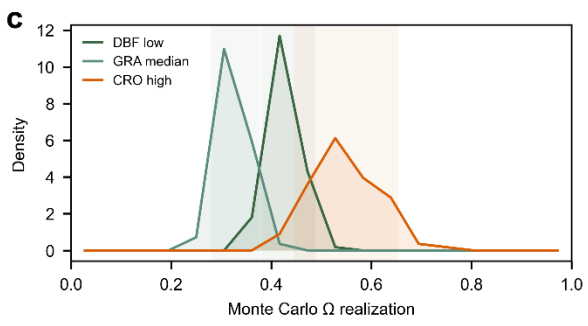
Fig. S3. Monte Carlo uncertainty propagation for the gridded Ω product.

a, Workflow of the Monte Carlo uncertainty propagation. Source-informed perturbations were applied to the gridded input drivers, Ω_{phys} was recomputed for each realization, and perturbed predictors were propagated through the PIML residual models. Pixel-level uncertainty was defined as the p95-p05 range of the resulting Monte Carlo Ω realizations. **b**, One-standard-deviation perturbation magnitudes assigned to the input drivers and physical parameters used in the uncertainty propagation. **c**, Example distributions of 100 Monte Carlo Ω realizations for representative low-, median-, and high-uncertainty pixels. Shaded intervals indicate the p05-p95 range. A wide distribution means the predicted Ω is more sensitive to input uncertainty. **d**, Convergence of Ω_{unc} with increasing Monte Carlo sample size, expressed relative to the 100-realization estimate. The solid line shows the median across diagnostic pixels, shading indicates the interquartile range, and the dashed line shows the mean.



b

Input or parameter	1 SD perturbation	Type
LE	max(5% x |value|, 5 W m^{-2})	additive
VPD	CV = 5%	multiplicative
R_g	CV = 4%	multiplicative
LAI	max(5% x |value|, 0.025)	additive
T_{air}	0.5 degC	additive
SWC	2.5	additive
WS	max(3% x |value|, 0.05 m s^{-1})	additive
CO_2	1 ppm	additive
Pr	CV = 10%	lognormal
Stomatal g_{max}	CV = 15%	lognormal
Radiation/VPD response	CV = 10%	lognormal
Thermal limits	0.5-1.0 degC	additive
Canopy height	CV = 3%	lognormal



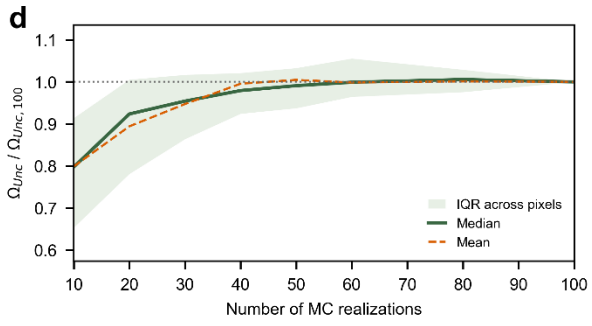


Figure S4. Patterns of Ω at site level in CONUS.

(a-e), The mean Ω values of different sites from the start year to the end year. Different colors correspond to PFTs. (**f**), The average values of different sites for different biomes. Different letters above the bars indicate significant differences among PFTs at the site level according to Tukey's test ($p < 0.05$).

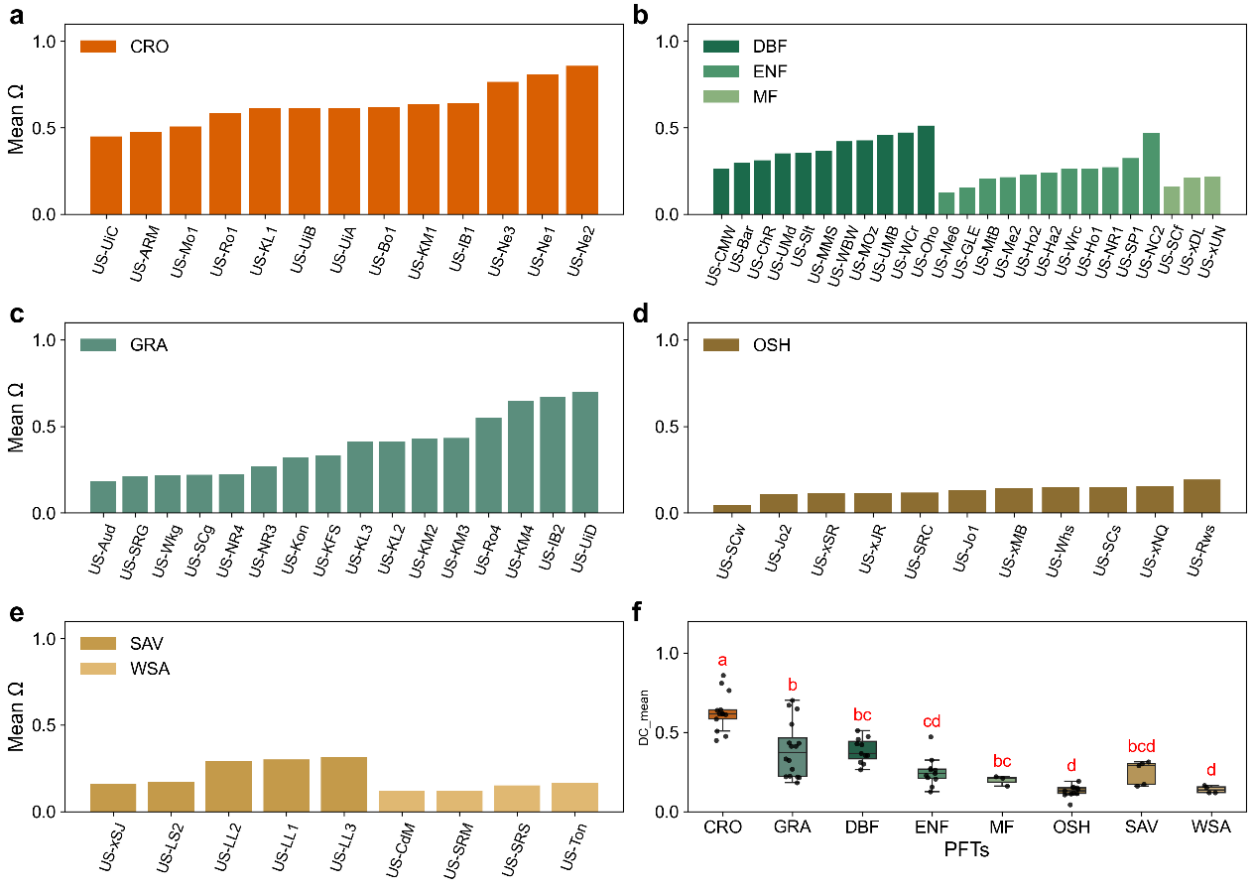


Figure S5. Site-level validation skill ranked across flux-tower sites.

Sites are ordered from highest to lowest site-level R^2 under site-blocked cross-validation. Bars represent individual sites and are colored by PFT. Site labels are abbreviated by removing the "US-" prefix.

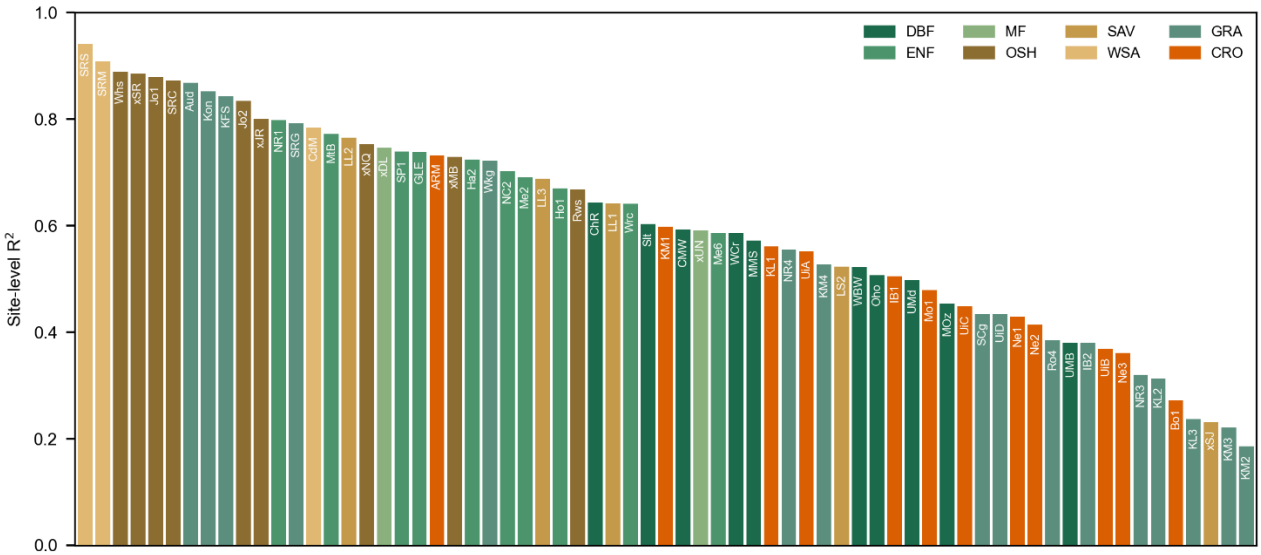


Figure S6. PFT-specific validation performance of the physical prior, Direct ML, and PIML. **a,** Out-of-fold R^2 for the calibrated physical prior, Direct ML, and PIML models across PFTs. **b,** Corresponding out-of-fold RMSE. Bars summarize the PFT-specific validation results from the site-blocked cross-validation outputs, with colors denoting modelling frameworks.

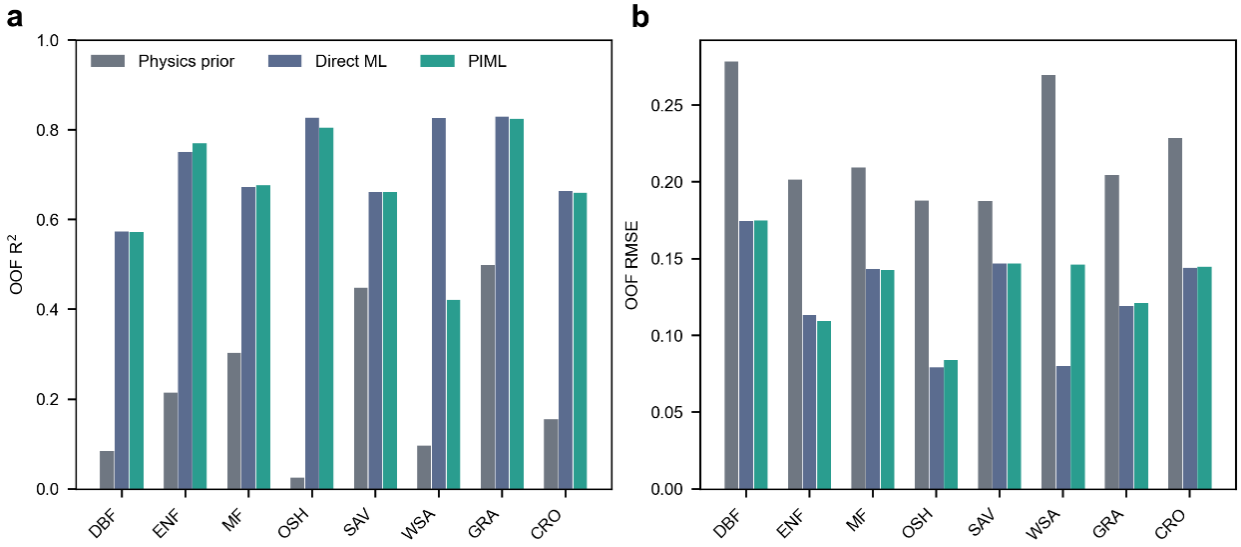


Figure S7. Site-level comparison between observed mean Ω and matched gridded product mean Ω.

a, Site mean observed Ω versus matched gridded annual mean Ω. Point size indicates the number of paired site-product years, and colors denote plant functional types. The 1:1 line is shown in black. **b**, Distribution of product bias, calculated as gridded minus observed site mean Ω, by PFT. **c**, Site-level annual Ω trend versus matched gridded annual Ω trend for long-record sites with at least 15 paired years. Trends are expressed as Ω decade^{-1}. **d**, Sensitivity of site-product trend correlation to the minimum number of paired years required for inclusion. Labels indicate the number of sites retained at each threshold.

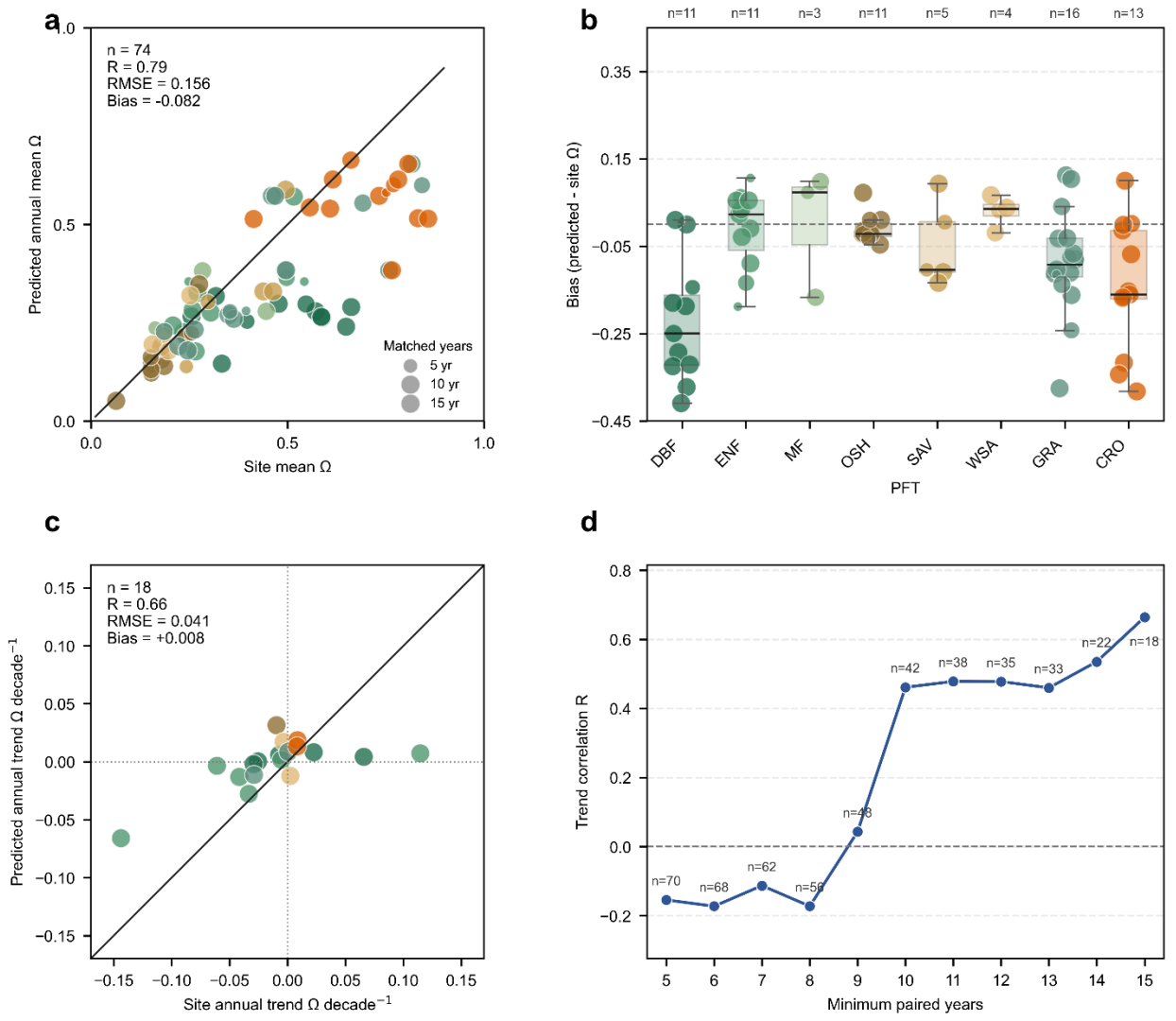


Figure S8. Continent full 8-day Ω time series by PFT-specific product.

a-h, PFT-specific Ω dynamics from 1982 to 2020 are shown at the native 8-day temporal resolution of the gridded product. Solid lines indicate the PFT-level mean Ω for each 8-day period, calculated from all valid target grid cells within the corresponding PFT. Shaded bands indicate the interquartile range across valid grid cells for each PFT and 8-day period. Colors are consistent with the PFT colors used throughout the manuscript.

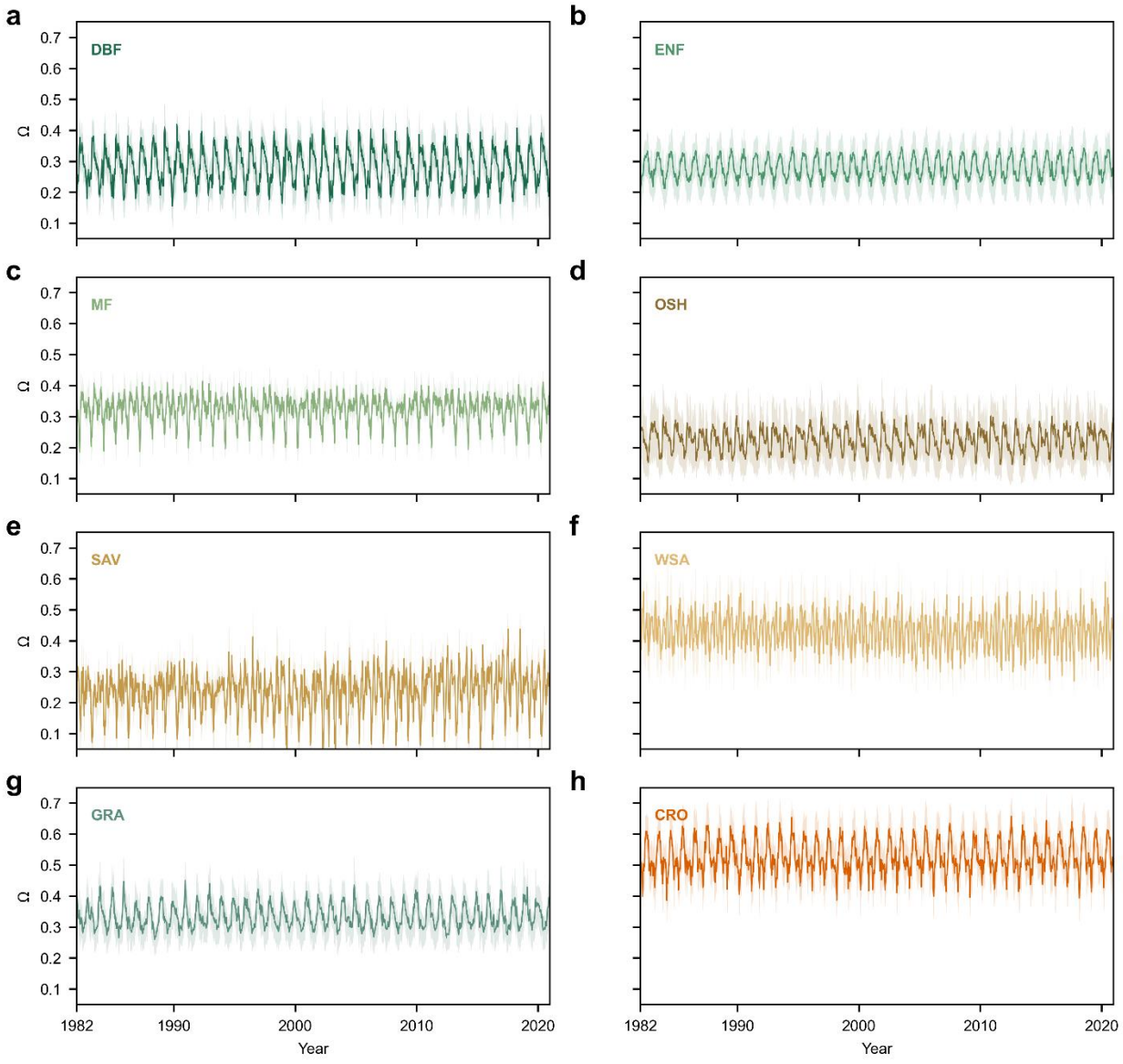


Figure S9. Continent PFT-specific annual mean Ω time series.

Annual mean Ω from 1982 to 2020 is shown separately for each PFT. Each panel represents one PFT, allowing temporal changes to be evaluated without pooling all grid cells across vegetation types. Reported slopes indicate linear trends in Ω per decade.

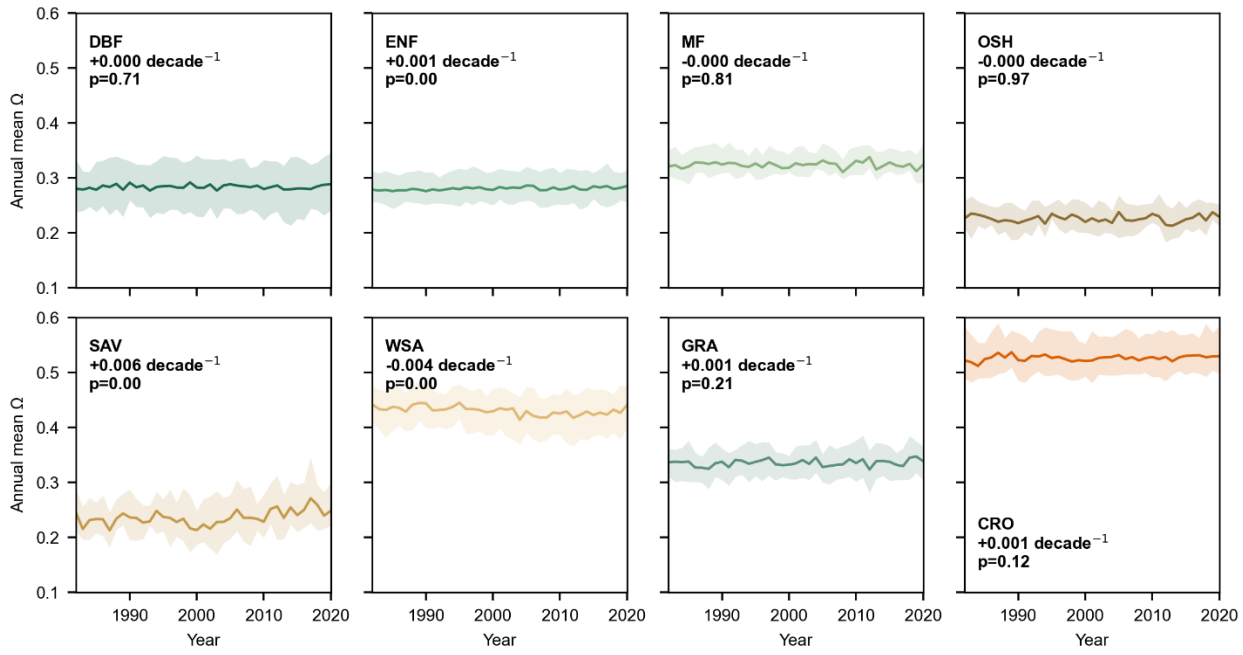


Figure S10. Spatial, seasonal, and interannual patterns of Monte Carlo uncertainty.

a, Mean Monte Carlo uncertainty of Ω across the CONUS product domain. **b**, Distribution of mean Monte Carlo uncertainty by PFT. **c**, Seasonal variation in mean uncertainty across 8-day periods. **d**, Interannual variation in mean uncertainty from 1982 to 2020.

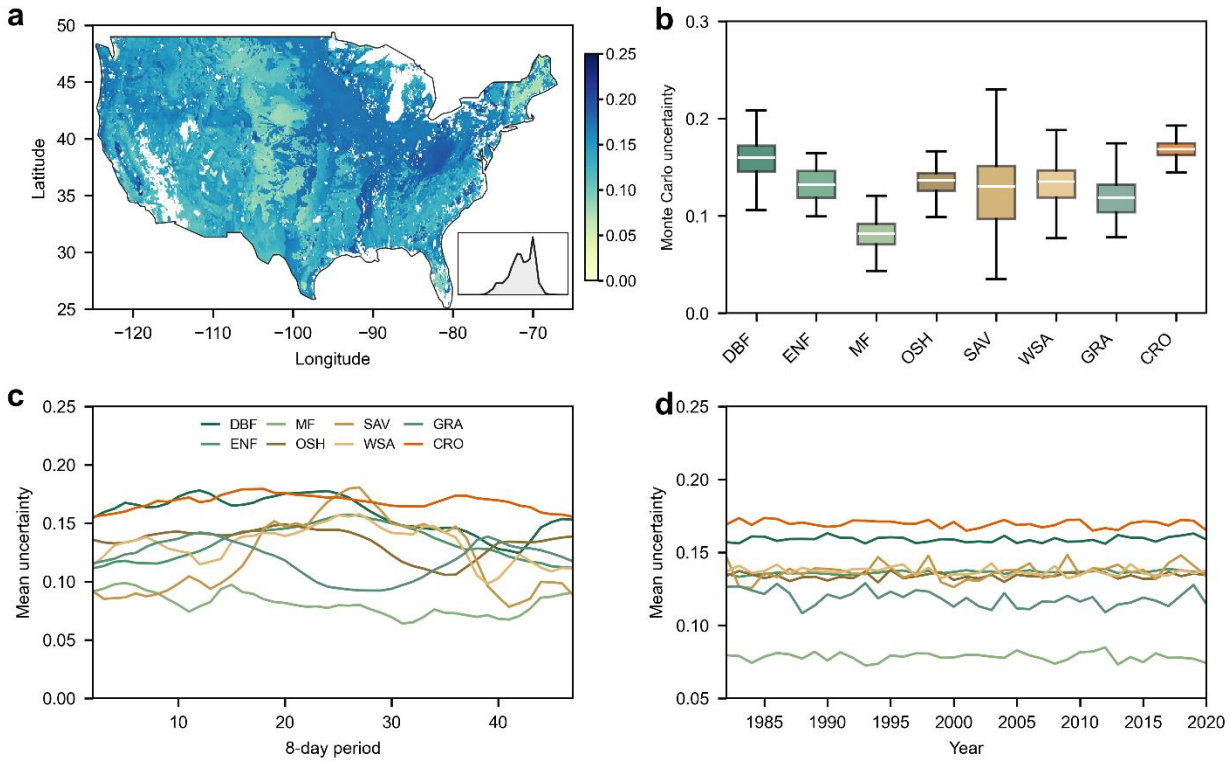


Figure S11. Annual quality-control composition and PFT-specific valid fraction.

(a) Annual percentage of target grid cells assigned to the four quality-control classes. For each year, quality-control classes were calculated from the 8-day QA layers of the current PIML product. "Low issue" indicates target grid cells with missing rate < 0.30 and pre-clipping outside-rate < 0.01; "Missing-prone" indicates missing rate ≥ 0.30; "Clipped-prone" indicates pre-clipping outside-rate ≥ 0.01; and "Mixed" indicates grid cells satisfying both missing-prone and clipped-prone criteria. (b) Annual valid fraction by PFT, calculated as the fraction of valid Ω estimates among all target PFT grid cells and 8-day periods within each year.

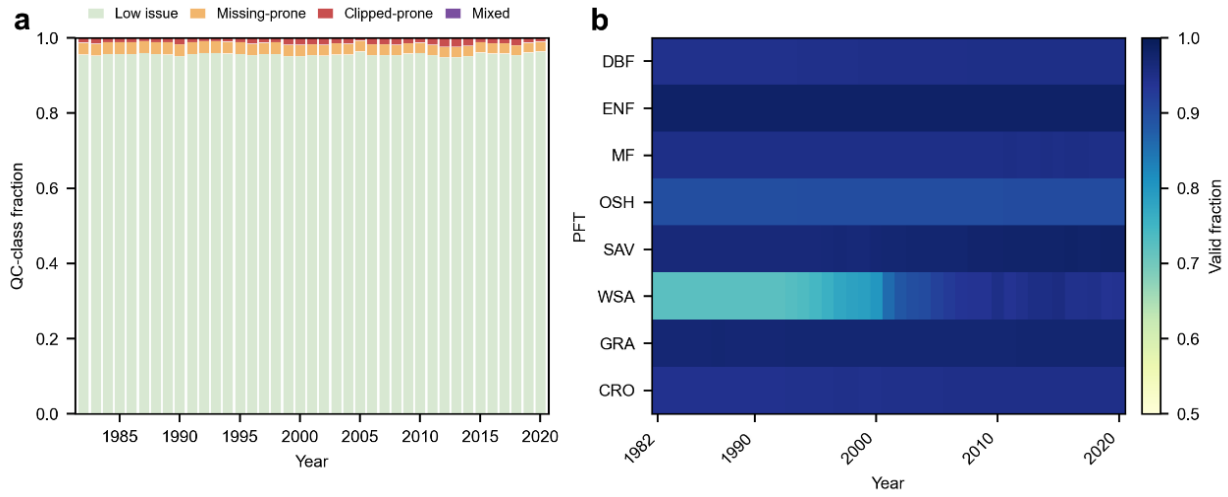


Figure S12. Sensitivity of the gridded Ω product to masking low-LAI periods.

Sensitivity analysis comparing the original PIML Ω product with a version in which grid-cell 8-day periods with missing LAI or LAI ≤ 0.1 were masked. **(a)** Annual mean Ω before and after LAI masking. **(b)** Annual fraction of valid Ω estimates removed by the LAI mask. **(c)** Mean PFT-level change in Ω after LAI masking, calculated as LAI-masked minus original Ω. **(d)** Change in PFT-level linear trend after LAI masking, expressed as Ω decade^{-1}. The small differences indicate that the main product-level conclusions were insensitive to low-LAI masking.

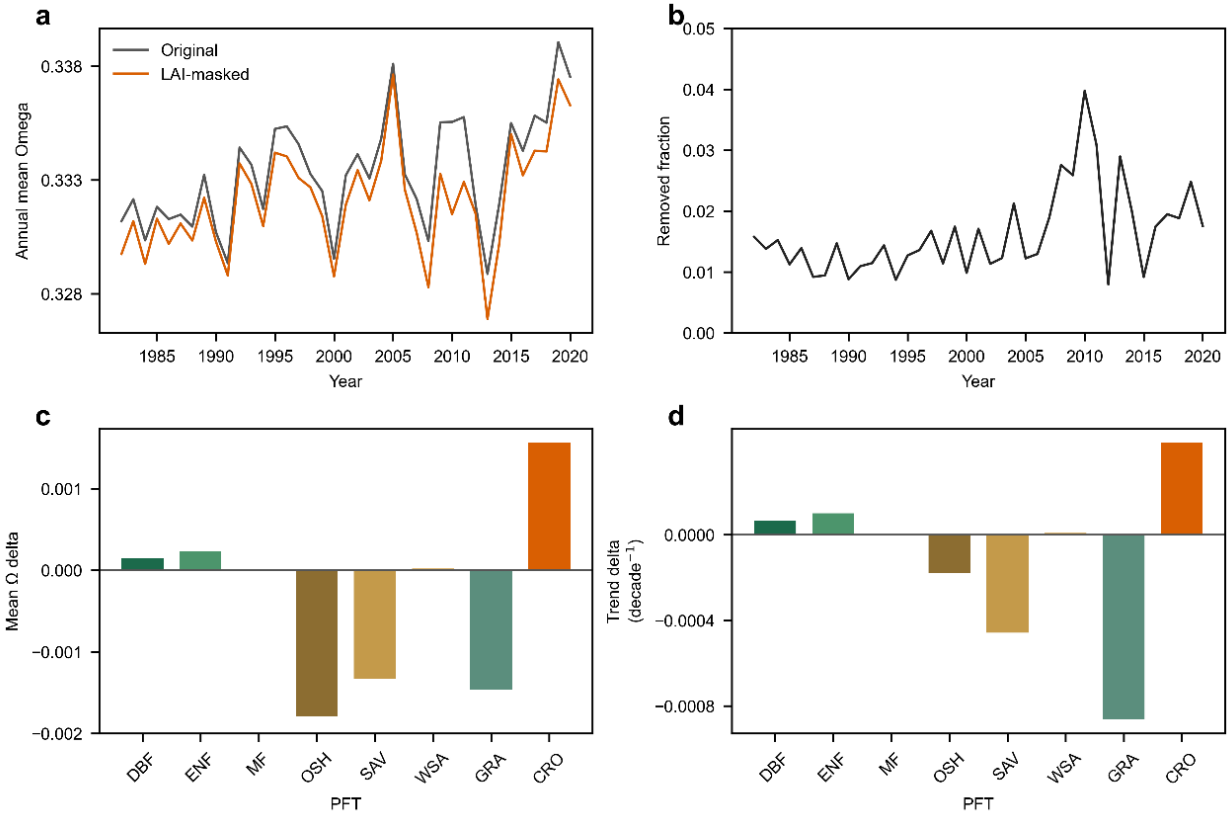


Table S1. Summary of site information.

Site ID	PFT	Lat	Lon	MAP	MAT	Valid years	Valid 8-day samples	Reference
US-ARM	CRO	36.6	-97.5	843	14.8	21	665	82
US-Bo1	CRO	40	-88.3	991.3	11	7	200	83
US-IB1	CRO	41.9	-88.2	929.2	9.2	12	340	84
US-KL1	CRO	42.5	-85.4	1027	9.9	13	303	85
US-KM1	CRO	42.4	-85.3	1027	9.9	13	321	86
US-Mo1	CRO	39.2	-92.1	981	12	10	305	87
US-Ne1	CRO	41.2	-96.5	790.4	10.1	22	168	88
US-Ne2	CRO	41.2	-96.5	788.9	10.1	13	158	89
US-Ne3	CRO	41.2	-96.4	783.7	10.1	11	105	90
US-Ro1	CRO	44.7	-93.1	879	6.4	3	104	91
US-UiA	CRO	40.1	-88.2	1051	10.9	6	138	92
US-UiB	CRO	40.1	-88.2	1051	10.9	11	118	93
US-UiC	CRO	40.1	-88.2	1051	10.9	14	377	94
US-Bar	DBF	44.1	-71.3	1245.8	5.6	20	319	95
US-CMW	DBF	31.7	-110.2	288	17	21	534	96
US-ChR	DBF	35.9	-84.3	1358.8	13.9	13	418	97
US-MMS	DBF	39.3	-86.4	1032	10.8	9	152	98
US-MOz	DBF	38.7	-92.2	986	12.1	17	364	99
US-Oho	DBF	41.6	-83.8	849	10.1	10	166	100
US-Slt	DBF	39.9	-74.6	1138	11	6	118	101
US-UMB	DBF	45.6	-84.7	803	5.8	14	225	102
US-UMd	DBF	45.6	-84.7	803	5.8	15	268	103
US-WBW	DBF	36	-84.3	1372	13.7	8	147	104
US-WCr	DBF	45.8	-90.1	787	4	20	277	105
US-GLE	ENF	41.4	-106.2	1200	0.8	15	289	106
US-Ha2	ENF	42.5	-72.2	1071	6.6	6	124	107
US-Ho1	ENF	45.2	-68.7	1070	5.3	3	107	108
US-Ho2	ENF	45.2	-68.7	1064	5.1	3	110	109
US-Me2	ENF	44.5	-121.6	523	6.3	21	768	110
US-Me6	ENF	44.3	-121.6	494	7.6	13	461	111
US-MtB	ENF	32.4	-110.7	790	9.3	15	566	112
US-NC2	ENF	35.8	-76.7	1320	16.6	19	601	113
US-NR1	ENF	40	-105.5	800	1.5	23	496	114
US-SP1	ENF	29.7	-82.2	1309.8	20.1	7	214	115
US-Wrc	ENF	45.8	-122	2452	8.8	15	479	116
US-Aud	GRA	31.6	-110.5	438.4	14.8	7	186	117
US-IB2	GRA	41.8	-88.2	930.2	9	14	142	118
US-KFS	GRA	39.1	-95.2	1014	12	9	234	119

US-KL2	GRA	42.5	-85.4	1027	9.9	13	561	120
US-KL3	GRA	42.5	-85.4	1027	9.9	13	533	121
US-KM2	GRA	42.4	-85.3	1027	9.9	13	537	122
US-KM3	GRA	42.4	-85.3	1027	9.9	13	518	123
US-KM4	GRA	42.4	-85.3	1027	9.9	12	148	124
US-Kon	GRA	39.1	-96.6	867	12.8	12	357	125
US-NR3	GRA	40.1	-105.6	884	-2.2	6	220	126
US-NR4	GRA	40.1	-105.6	884	-2.2	3	105	127
US-Ro4	GRA	44.7	-93.1	879	6.4	8	184	128
US-SCg	GRA	33.7	-117.7			9	269	129
US-SRG	GRA	31.8	-110.8	420	17	16	565	130
US-UiD	GRA	40.1	-88.2	1051	10.9	7	126	131
US-Wkg	GRA	31.7	-109.9	407	15.6	21	647	132
US-Jo1	OSH	32.6	-106.6	245.1	14.7	13	394	133
US-Jo2	OSH	32.6	-106.6	282.3	17.5	11	389	134
US-Rws	OSH	43.2	-116.7	290	8.9	9	364	135
US-SCs	OSH	33.7	-117.7			10	274	136
US-SCw	OSH	33.6	-116.5			10	313	137
US-SRC	OSH	31.9	-110.8	330	22	7	211	138
US-Whs	OSH	31.7	-110.1	320	17.6	19	846	139
US-xJR	OSH	32.6	-106.8	271.3	15.7	8	229	140
US-xMB	OSH	38.2	-109.4	319.5	10.1	7	237	141
US-xNQ	OSH	40.2	-112.5	288.3	9	6	205	142
US-xSR	OSH	31.9	-110.8	346	19.3	7	247	143
US-LL1	SAV	31.3	-84.5	1310	20	12	520	144
US-LL2	SAV	31.2	-84.4	1310	20	9	397	145
US-LL3	SAV	31.3	-84.5	1310	20	9	394	146
US-LS2	SAV	31.6	-110.1	288	17	5	190	147
US-xSJ	SAV	37.1	-119.7	539.6	16.4	6	227	148
US-CdM	WSA	37.5	-109.7	348	11.3	7	174	149
US-SRM	WSA	31.8	-110.9	380	17.9	22	986	150
US-SRS	WSA	31.8	-110.9	388	19.4	8	266	151
US-Ton	WSA	38.4	-121	559	15.8	25	1065	152
US-SCf	MF	33.8	-116.8			5	144	153
US-xDL	MF	32.5	-87.8	1372	17.6	8	274	154
US-xUN	MF	46.2	-89.5	802.3	4.3	8	242	155

Table S2. Crosswalk between the ESA CCI land-cover classes and the plant functional types used in this study.

PFT	IGBP	ESA CCI class codes	Corresponding ESA CCI land-cover classes
CRO	Croplands	10, 11, 12, 20, 30	Rainfed cropland; herbaceous cropland; tree or shrub cropland; irrigated or post-flooding cropland; cropland-dominated mosaic
GRA	Grasslands	130	Grassland
ENF	Evergreen needleleaf forests	70, 71, 72	Evergreen needleleaf tree cover, including closed and open classes
DBF	Deciduous broadleaf forests	60, 61, 62	Deciduous broadleaf tree cover, including closed and open classes
WSA	Woody savannas	100, 151	Tree- and shrub-dominated mosaic; sparse tree cover
OSH	Open shrublands	120, 121, 122	Shrubland, evergreen shrubland, and deciduous shrubland
SAV	Savannas	110, 150, 153	Herbaceous-dominated mosaic with trees or shrubs; sparse vegetation; sparse herbaceous cover
MF	Mixed forests	90	Mixed broadleaf and needleleaf tree cover

Table S3. Summary of site, satellite, and reanalysis datasets, and auxiliary validation datasets.

Variable	Dataset	Period	Original resolution	Final resolution	Role
R_g, T_{dew}, T_a, WS, Pr and SWC	ERA5-Land	1982–2020	0.1°, daily	0.1°, 8-day	Predictor/Ω_{phy}
ET	GLEAM	1982–2020	0.1°, daily	0.1°, 8-day	Predictor
ET	GLASS	1982–2020	0.05°, 8-day	0.1°, 8-day	Predictor
Land Cover	ESA_CCI	1992–2020	300m, annual	0.1°, annual	PFT mask
LAI	GIMMS LAI4g	1982–2020	Half-monthly	0.1°, 8-day	Predictor
Tree height	Dataset from Potapov et al., 2021	2019	30m	–	Ω_{phy}
Tree age	GAMI v2	2020	100m	–	Ω_{phy}
CO_2	NOAA	1982–2020	daily	8-day	Predictor

References

82. Sebastien Biraud, Marc Fischer, Stephen Chan, Margaret Torn (2026), AmeriFlux BASE US-ARM ARM Southern Great Plains site- Lamont, Ver. 15-5, AmeriFlux AMP, (Dataset). https://doi.org/10.17190/AMF/1246027
83. Tilden Meyers (2016), AmeriFlux BASE US-Bo1 Bondville, Ver. 2-1, AmeriFlux AMP, (Dataset). https://doi.org/10.17190/AMF/1246036
84. Roser Matamala (2019), AmeriFlux BASE US-IB1 Fermi National Accelerator Laboratory-Batavia (Agricultural site), Ver. 8-5, AmeriFlux AMP, (Dataset). https://doi.org/10.17190/AMF/1246065
85. Philip Robertson, Jiquan Chen (2025), AmeriFlux BASE US-KL1 KBS Lux Arbor Reserve Corn, Ver. 4-5, AmeriFlux AMP, (Dataset). https://doi.org/10.17190/AMF/1660344
86. Philip Robertson, Jiquan Chen (2022), AmeriFlux BASE US-KM1 KBS Marshall Farms Corn, Ver. 4-5, AmeriFlux AMP, (Dataset). https://doi.org/10.17190/AMF/1647439
87. Adam Schreiner-McGraw (2026), AmeriFlux BASE US-Mo1 LTAR CMRB Field 1 (CMRB ASP), Ver. 5-5, AmeriFlux AMP, (Dataset). https://doi.org/10.17190/AMF/1870588
88. Andy Suyker (2025), AmeriFlux BASE US-Ne1 Mead - irrigated continuous maize site, Ver. 19-5, AmeriFlux AMP, (Dataset). https://doi.org/10.17190/AMF/1246084
89. Andy Suyker (2025), AmeriFlux BASE US-Ne2 Mead - irrigated maize-soybean rotation site, Ver. 19-5, AmeriFlux AMP, (Dataset). https://doi.org/10.17190/AMF/1246085
90. Andy Suyker (2025), AmeriFlux BASE US-Ne3 Mead - rainfed maize-soybean rotation site, Ver. 19-5, AmeriFlux AMP, (Dataset). https://doi.org/10.17190/AMF/1246086
91. John Baker, Tim Griffis, Timothy Griffis (2018), AmeriFlux BASE US-Ro1 Rosemount- G21, Ver. 5-5, AmeriFlux AMP, (Dataset). https://doi.org/10.17190/AMF/1246092
92. Carl Bernacchi, Bethany Blakely, Caitlin Moore, Taylor Pederson (2025), AmeriFlux BASE US-UiA University of Illinois Switchgrass, Ver. 3-5, AmeriFlux AMP, (Dataset). https://doi.org/10.17190/AMF/1617725
93. Carl J Bernacchi, Bethany Blakely, Caitlin Moore, Taylor Pederson (2025), AmeriFlux BASE US-UiB University of Illinois Miscanthus, Ver. 3-5, AmeriFlux AMP, (Dataset).

https://doi.org/10.17190/AMF/1846664

94. Carl J Bernacchi, Bethany Blakely, Caitlin Moore, Taylor Pederson (2025), AmeriFlux BASE US-UiC University of Illinois Maize-Soy, Ver. 2-5, AmeriFlux AMP, (Dataset). https://doi.org/10.17190/AMF/1846665
95. Andrew Richardson, David Hollinger (2025), AmeriFlux BASE US-Bar Bartlett Experimental Forest, Ver. 7-5, AmeriFlux AMP, (Dataset). https://doi.org/10.17190/AMF/1246030
96. Russell Scott (2025), AmeriFlux BASE US-CMW Charleston Mesquite Woodland, Ver. 3-5, AmeriFlux AMP, (Dataset). https://doi.org/10.17190/AMF/1660339
97. Ivan Mauricio Cely-Toro, Praveena Krishnan, Rick Saylor, John Kochendorfer, Tilden Meyers (2025), AmeriFlux BASE US-ChR Chestnut Ridge, Ver. 3-5, AmeriFlux AMP, (Dataset). https://doi.org/10.17190/AMF/1246044
98. Kim Novick, Rich Phillips (2026), AmeriFlux BASE US-MMS Morgan Monroe State Forest, Ver. 32-5, AmeriFlux AMP, (Dataset). https://doi.org/10.17190/AMF/1246080
99. Jeffrey Wood, Lianhong Gu (2022), AmeriFlux BASE US-MOz Missouri Ozark Site, Ver. 11-5, AmeriFlux AMP, (Dataset). https://doi.org/10.17190/AMF/1246081
100. Jiquan Chen, Housen Chu, Asko Noormets (2021), AmeriFlux BASE US-Oho Oak Openings, Ver. 7-5, AmeriFlux AMP, (Dataset). https://doi.org/10.17190/AMF/1246089
101. Gallagher (2026), AmeriFlux BASE US-Slt Silas Little- New Jersey, Ver. 8-5, AmeriFlux AMP, (Dataset). https://doi.org/10.17190/AMF/1246096
102. Aimee Classen, Christopher Gough, Gil Bohrer, John Lenters, Peter Curtis (2026), AmeriFlux BASE US-UMB Univ. of Mich. Biological Station, Ver. 25-5, AmeriFlux AMP, (Dataset). https://doi.org/10.17190/AMF/1246107
103. Aimee Classen, Christopher Gough, Gil Bohrer, John Lenters, Peter Curtis (2025), AmeriFlux BASE US-UMd UMBS Disturbance, Ver. 19-5, AmeriFlux AMP, (Dataset). https://doi.org/10.17190/AMF/1246134
104. Tilden Meyers (2016), AmeriFlux BASE US-WBW Walker Branch Watershed, Ver. 2-1, AmeriFlux AMP, (Dataset). https://doi.org/10.17190/AMF/1246109

105. Ankur Desai, Ankur Desai (2026), AmeriFlux BASE US-WCr Willow Creek, Ver. 35-5, AmeriFlux AMP, (Dataset). https://doi.org/10.17190/AMF/1246111
106. John Frank, George Valentine, Bill Massman (2026), AmeriFlux BASE US-GLE GLEES, Ver. 9-5, AmeriFlux AMP, (Dataset). https://doi.org/10.17190/AMF/1246056
107. William Munger (2026), AmeriFlux BASE US-Ha2 Harvard Forest Hemlock Site, Ver. 16-5, AmeriFlux AMP, (Dataset). https://doi.org/10.17190/AMF/1246060
108. Andrew Ouimette, Roel Ruzol (2026), AmeriFlux BASE US-Ho1 Howland Forest (main tower), Ver. 15-5, AmeriFlux AMP, (Dataset). https://doi.org/10.17190/AMF/1246061
109. Andrew Ouimette, Roel Ruzol (2026), AmeriFlux BASE US-Ho2 Howland Forest (west tower), Ver. 10-5, AmeriFlux AMP, (Dataset). https://doi.org/10.17190/AMF/1246062
110. Chad Hanson, Chris Still, Bev Law (2026), AmeriFlux BASE US-Me2 Metolius mature ponderosa pine, Ver. 23-5, AmeriFlux AMP, (Dataset). https://doi.org/10.17190/AMF/1246076
111. Chad Hanson, Chris Still, Bev Law (2026), AmeriFlux BASE US-Me6 Metolius Young Pine Burn, Ver. 20-5, AmeriFlux AMP, (Dataset). https://doi.org/10.17190/AMF/1246128
112. Greg Barron-Gafford (2025), AmeriFlux BASE US-MtB Mt Bigelow, Ver. 5-5, AmeriFlux AMP, (Dataset). https://doi.org/10.17190/AMF/1579717
113. Asko Noormets, Ge Sun, Michael Gavazzi, Jean-Christophe Domec, Steve McNulty, Guofang Miao, Maricar Aguilos, Bhaskar Mitra, Kevan Minick, John King, Benju Baniya, Jiaojiao Dong, Linqing Yang, Miko Lorenzo Belgado, Prajaya Prajapati (2026), AmeriFlux BASE US-NC2 NC_Loblolly Plantation, Ver. 22-5, AmeriFlux AMP, (Dataset). https://doi.org/10.17190/AMF/1246083
114. Peter D. Blanken, Russel K. Monson, Sean P. Burns, David R. Bowling, Andrew A. Turnipseed, John F. Knowles (2026), AmeriFlux BASE US-NR1 Niwot Ridge Forest (LTER NWT1), Ver. 26-5, AmeriFlux AMP, (Dataset). https://doi.org/10.17190/AMF/1246088
115. Rosvel Bracho, Timothy A. Martin (2023), AmeriFlux BASE US-SP1 Slashpine-Austin Cary-65yrs nat regen, Ver. 5-5, AmeriFlux AMP, (Dataset). https://doi.org/10.17190/AMF/1246100

116. Sonia Wharton (2016), AmeriFlux BASE US-Wrc Wind River Crane Site, Ver. 8-1, AmeriFlux AMP, (Dataset). https://doi.org/10.17190/AMF/1246114
117. Praveena Krishnan, John Kochendorfer, Tilden Meyers (2025), AmeriFlux BASE US-Aud Audubon Research Ranch, Ver. 5-5, AmeriFlux AMP, (Dataset). https://doi.org/10.17190/AMF/1246028
118. Roser Matamala (2019), AmeriFlux BASE US-IB2 Fermi National Accelerator Laboratory-Batavia (Prairie site), Ver. 8-5, AmeriFlux AMP, (Dataset). https://doi.org/10.17190/AMF/1246066
119. Nathaniel Brunsell (2020), AmeriFlux BASE US-KFS Kansas Field Station, Ver. 7-5, AmeriFlux AMP, (Dataset). https://doi.org/10.17190/AMF/1246132
120. Philip Robertson, Jiquan Chen (2022), AmeriFlux BASE US-KL2 KBS Lux Arbor Reserve Switchgrass, Ver. 4-5, AmeriFlux AMP, (Dataset). https://doi.org/10.17190/AMF/1644212
121. Philip Robertson, Jiquan Chen (2022), AmeriFlux BASE US-KL3 KBS Lux Arbor Reserve Prairie, Ver. 4-5, AmeriFlux AMP, (Dataset). https://doi.org/10.17190/AMF/1647438
122. Philip Robertson, Jiquan Chen (2022), AmeriFlux BASE US-KM2 KBS Marshall Farms Prairie, Ver. 4-5, AmeriFlux AMP, (Dataset). https://doi.org/10.17190/AMF/1647440
123. Philip Robertson, Jiquan Chen (2022), AmeriFlux BASE US-KM3 KBS Marshall Farms Switchgrass, Ver. 3-5, AmeriFlux AMP, (Dataset). https://doi.org/10.17190/AMF/1660345
124. Philip Robertson, Jiquan Chen (2022), AmeriFlux BASE US-KM4 KBS Marshall Farms Smooth Brome Grass (Ref), Ver. 5-5, AmeriFlux AMP, (Dataset). https://doi.org/10.17190/AMF/1634882
125. Nathaniel Brunsell (2020), AmeriFlux BASE US-Kon Konza Prairie LTER (KNZ), Ver. 5-5, AmeriFlux AMP, (Dataset). https://doi.org/10.17190/AMF/1246068
126. John Knowles (2025), AmeriFlux BASE US-NR3 Niwot Ridge Alpine (T-Van West), Ver. 6-5, AmeriFlux AMP, (Dataset). https://doi.org/10.17190/AMF/1804491
127. John Knowles (2025), AmeriFlux BASE US-NR4 Niwot Ridge Alpine (T-Van East), Ver. 6-5, AmeriFlux AMP, (Dataset). https://doi.org/10.17190/AMF/1804492

128. John Baker, Tim Griffis (2026), AmeriFlux BASE US-Ro4 Rosemount Prairie, Ver. 32-5, AmeriFlux AMP, (Dataset). https://doi.org/10.17190/AMF/1419507
129. Mike Goulden (2018), AmeriFlux BASE US-SCg Southern California Climate Gradient - Grassland, Ver. 1-5, AmeriFlux AMP, (Dataset). https://doi.org/10.17190/AMF/1419502
130. Russell Scott (2026), AmeriFlux BASE US-SRG Santa Rita Grassland, Ver. 20-5, AmeriFlux AMP, (Dataset). https://doi.org/10.17190/AMF/1246154
131. Carl Bernacchi (2023), AmeriFlux BASE US-UiD University of Illinois Restored Native Prairie, Ver. 1-5, AmeriFlux AMP, (Dataset). https://doi.org/10.17190/AMF/1987605
132. Russell Scott (2026), AmeriFlux BASE US-Wkg Walnut Gulch Kendall Grasslands, Ver. 27-5, AmeriFlux AMP, (Dataset). https://doi.org/10.17190/AMF/1246112
133. Craig Tweedie (2024), AmeriFlux BASE US-Jo1 Jornada Experimental Range Bajada Site, Ver. 4-5, AmeriFlux AMP, (Dataset). https://doi.org/10.17190/AMF/1767833
134. Enrique R. Vivoni, Eli R. Perez-Ruiz (2022), AmeriFlux BASE US-Jo2 Jornada Experimental Range Mixed Shrubland, Ver. 2-5, AmeriFlux AMP, (Dataset). https://doi.org/10.17190/AMF/1617696
135. Gerald Flerchinger (2025), AmeriFlux BASE US-Rws Reynolds Creek Wyoming big sagebrush, Ver. 7-5, AmeriFlux AMP, (Dataset). https://doi.org/10.17190/AMF/1375201
136. Mike Goulden (2018), AmeriFlux BASE US-SCs Southern California Climate Gradient - Coastal Sage, Ver. 1-5, AmeriFlux AMP, (Dataset). https://doi.org/10.17190/AMF/1419501
137. Mike Goulden (2018), AmeriFlux BASE US-SCw Southern California Climate Gradient - Pinyon/Juniper Woodland, Ver. 1-5, AmeriFlux AMP, (Dataset). https://doi.org/10.17190/AMF/1419504
138. Shirley Kurc (2019), AmeriFlux BASE US-SRC Santa Rita Creosote, Ver. 6-5, AmeriFlux AMP, (Dataset). https://doi.org/10.17190/AMF/1246127
139. Russell Scott (2026), AmeriFlux BASE US-Whs Walnut Gulch Lucky Hills Shrub, Ver. 27-5, AmeriFlux AMP, (Dataset). https://doi.org/10.17190/AMF/1246113
140. NEON (National Ecological Observatory Network) (2025), AmeriFlux BASE US-xJR NEON

Jornada LTER (JORN), Ver. 10-5, AmeriFlux AMP, (Dataset). https://doi.org/10.17190/AMF/1617731

141. NEON (National Ecological Observatory Network) (2025), AmeriFlux BASE US-xMB NEON Moab (MOAB), Ver. 9-5, AmeriFlux AMP, (Dataset). https://doi.org/10.17190/AMF/1671896

142. NEON (National Ecological Observatory Network) (2025), AmeriFlux BASE US-xNQ NEON Onaqui-Ault (ONAQ), Ver. 10-5, AmeriFlux AMP, (Dataset). https://doi.org/10.17190/AMF/1617733

143. NEON (National Ecological Observatory Network) (2025), AmeriFlux BASE US-xSR NEON Santa Rita Experimental Range (SRER), Ver. 10-5, AmeriFlux AMP, (Dataset). https://doi.org/10.17190/AMF/1579543

144. Gregory Starr (2021), AmeriFlux BASE US-LL1 Longleaf Pine - Baker (Mesic site), Ver. 2-5, AmeriFlux AMP, (Dataset). https://doi.org/10.17190/AMF/1773395

145. Gregory Starr (2021), AmeriFlux BASE US-LL2 Longleaf Pine - Dubignion (Intermediate site), Ver. 1-5, AmeriFlux AMP, (Dataset). https://doi.org/10.17190/AMF/1773396

146. Gregory Starr (2021), AmeriFlux BASE US-LL3 Longleaf Pine - Red Dirt (Xeric site), Ver. 1-5, AmeriFlux AMP, (Dataset). https://doi.org/10.17190/AMF/1773397

147. Russell Scott (2025), AmeriFlux BASE US-LS2 San Pedro River Lewis Springs Savanna, Ver. 2-5, AmeriFlux AMP, (Dataset). https://doi.org/10.17190/AMF/1660347

148. NEON (National Ecological Observatory Network) (2025), AmeriFlux BASE US-xSJ NEON San Joaquin Experimental Range (SJER), Ver. 9-5, AmeriFlux AMP, (Dataset). https://doi.org/10.17190/AMF/1671901

149. David Bowling, Steve Kannenberg, William Anderegg (2026), AmeriFlux BASE US-CdM Cedar Mesa, Ver. 4-5, AmeriFlux AMP, (Dataset). https://doi.org/10.17190/AMF/1865477

150. Russell Scott (2026), AmeriFlux BASE US-SRM Santa Rita Mesquite, Ver. 31-5, AmeriFlux AMP, (Dataset). https://doi.org/10.17190/AMF/1246104

151. Enrique R. Vivoni, Eli R. Perez-Ruiz (2022), AmeriFlux BASE US-SRS Santa Rita Savanna,

Ver. 3-5, AmeriFlux AMP, (Dataset). https://doi.org/10.17190/AMF/1660351

152. Siyan Ma, Liukang Xu, Joseph Verfaillie, Dennis Baldocchi (2026), AmeriFlux BASE US-Ton Tonzi Ranch, Ver. 26-5, AmeriFlux AMP, (Dataset). https://doi.org/10.17190/AMF/1245971

153. Mike Goulden (2018), AmeriFlux BASE US-SCf Southern California Climate Gradient - Oak/Pine Forest, Ver. 1-5, AmeriFlux AMP, (Dataset). https://doi.org/10.17190/AMF/1419503

154. NEON (National Ecological Observatory Network) (2025), AmeriFlux BASE US-xDL NEON Dead Lake (DELA), Ver. 10-5, AmeriFlux AMP, (Dataset). https://doi.org/10.17190/AMF/1579721

155. NEON (National Ecological Observatory Network) (2025), AmeriFlux BASE US-xUN NEON University of Notre Dame Environmental Research Center (UNDE), Ver. 10-5, AmeriFlux AMP, (Dataset). https://doi.org/10.17190/AMF/1617741